

Structural control on the stability of overhanging, discontinuous rock slopes

Tsesarsky, M¹. and Hatzor Y. H

Department of Geological and Environmental Sciences. Ben Gurion University of the Negev. Beer-Sheva 84105, Israel

Leviathan, I.

Leviathan Engineers LTD. 8 Zichron Yakov St. Tel-Aviv 62999, Israel

Saltzman, U.

Engineering Geology and Rock Mechanics. 8a HaMelakha St. Ramat-Gan 52526, Israel

Sokolowksy, M.

Office of Geotechnical and Foundation Engineering. Administration of Engineering and Planning, Ministry of Construction and Housing, Israel.

Copyright 2005, ARMA, American Rock Mechanics Association

This paper was prepared for presentation at Alaska Rocks 2005, The 40th U.S. Symposium on Rock Mechanics (USRMS): Rock Mechanics for Energy, Mineral and Infrastructure Development in the Northern Regions, held in Anchorage, Alaska, June 25-29, 2005.

This paper was selected for presentation by a USRMS Program Committee following review of information contained in an abstract submitted earlier by the author(s). Contents of the paper, as presented, have not been reviewed by ARMA/USRMS and are subject to correction by the author(s). The material, as presented, does not necessarily reflect any position of USRMS, ARMA, their officers, or members. Electronic reproduction, distribution, or storage of any part of this paper for commercial purposes without the written consent of ARMA is prohibited. Permission to reproduce in print is restricted to an abstract of not more than 300 words; illustrations may not be copied. The abstract must contain conspicuous acknowledgement of where and by whom the paper was presented.

ABSTRACT: Instability of overhanging cliffs depends mainly on rock mass structure and on tensile stresses that develop at the base of the slope. In this paper we present stability analysis of a 34m high overhanging cliff, transected by closely spaced horizontal beddings and three sets of vertical joints. The upper third of the cliff is cantilevered and extrudes more than 11m beyond the toe of the slope, giving rise to eccentric loading at the base of the slope and buildup of tensile stresses within the rock mass. Field observations suggest that the vertical joints which transect the entire cliff form "tension cracks" at the back of the cliff, but their distance from the face is uncertain. Yet, the nature of deformation depends upon the exact location of the vertical tensile crack. The stability of the cliff under different geometrical configurations was studied using continuous 2-D FEA and 2-D Discontinuous Deformation Analysis. Both FEA and DDA are shown to agree with field observations. Based on computational results rock bolt reinforcement was added to the DDA model. Optimal reinforcement scheme was determined using kinematical based criterions.

1. INTRODUCTION

The stability of rock slopes is typically controlled by the rock mass structure, namely by the orientation, extent and density of the discontinuities in the slope. In a rock slope where the discontinuities do not dip out into the excavation space deformation and failure may be controlled by complex processes such as tilting, sliding, and block rotation. In cases where the rock mass contains sub-vertical joints columns of massive rock blocks may form and rotational movement may ensue [1]. Rotational failures can be broadly classified into two categories: 1) slumping – backward rotation; and 2) toppling – forward rotation [2]. Slumping occurs where sub-vertical joints dip towards the excavation space but do not "daylight" whereas

toppling occurs where sub-vertical joints dip into the rock. A comprehensive review of failure modes in rock slopes is presented by Goodman and Kiefer [2].

Stability analyses for rock slopes can be broadly classified in to two main categories: 1) Limit Equilibrium Methods (LEM) and 2) Numerical Methods. For failure in rotation several LEM techniques are available: Janbu simplified method [3], Bishop's method [4] and Wittke's method [5] can be used for slumping, the Goodman and Bray method [6] can be used for toppling. The main disadvantages of LEM are: 1) kinematics is not accounted for; and 2) the failure mode is assumed in advance, prior to analysis.

Numerical methods such as the Finite Element Method (FEM) or the discontinuous Discrete Element Method (DEM) are effective in the solution of complex problems and are also capable of simulating coupled processes. Whereas the

¹ Currently with the Faculty of Civil and Environmental Engineering, Technion – Israel Institute of Technology, Haifa 32000, Israel.

continuum based FEM is mainly suitable for slope stability analysis in soils and weak or highly altered rock which may be modeled as a continuum, the DEM is most suitable for analysis of structurally controlled instabilities. Numerical analysis offers many advantages over the traditional LEM, for example: 1) nonlinear behavior can be modeled; 2) complex geometries of slope and discontinuity network can be accounted for; 3) the failure mode need not be assumed in advance; 4) complex loading conditions may be modeled, 5) various initial and boundary conditions may be imposed.

An accurate description of the network formed by intersecting discontinuities is a fundamental problem of rock engineering in general and of slope stability analysis in particular. In most cases, the persistence of discontinuities and their termination within the rock mass are unknown. Surface survey techniques for persistence estimation have been suggested [e.g. 7, 8], but valid procedures for predictions of in-depth geometry are still not available. The geometric uncertainty is further augmented where the rock mass structure is partially or completely concealed by urban development, or when the effect of previous blasting and quarrying are unknown.

An effective geological description of any given problem should result in effective remedial engineering: i.e. transforming geological description into design oriented parameters. In the general case of slope stability the geometrical uncertainties of the rock mass structure should be related to engineering parameters such as displacements or loads.

In this paper we present a stability analysis of an overhanging cliff built of densely jointed rock, with an emphasis on kinematics. Stability analysis is performed using FEM, and an implicit DEM: the Discontinuous Deformation Analysis - DDA [9]. Based on the results of the numerical analysis rock bolt reinforcement is modeled using DDA and the effect of reinforcement on slope deformation is studied. The limitations of different analysis methods are discussed, and practical recommendations for stability analysis of overhanging cliffs are presented.

2. DESCRIPTION OF CASE STUDY

The studied cliff was formed due to quarrying activities in the early fifties. The cliff strikes SSW

to azimuth 185°, with local variations in strike which form large extrados. At places past quarrying activity and natural receding of the cliff base give rise to large overhangs, which cantilever beyond the base of the cliff. Field observations indicate that at certain areas along the cliff deformation is taking place. It seems that most of the deformation is taking place where the cliff is overhanging. Geological reconnaissance delimited the stability analysis to a particular section of the cliff which is 34m high and where the upper third of the cliff is cantilevered, and extrudes more than 11m beyond the toe of the slope.

The rock is comprised of a well bedded dolostone sequence. Bed thickness ranges between 5cm to 1.5m. Thick beds are formed generally as a result of a unification of several thinner beds. Chalk forms a secondary constituent throughout the otherwise dolostone mass, reaching 10-20% by volume. The thickness of chalk beds does not exceed several cm'. Chalk beds are not continuous, therefore, most of the mass shows mating contacts between dolostone beds.

The rock mass is transected by 4 sets of, sub-vertical joints. The attitude of three sets is oblique to the face of the cliff, whereas the fourth is parallel to excavation face. Mean orientation, dip and spacing for the different joint sets and bedding planes are presented in Table 1.

Table 1. Principal joint sets.

Joint set	Dip (°)	Dip Direction (°)	Spacing (m)
J1	7	272	0.8
J2	87	054	0.6
J3	88	184	0.9
J4	90	146	0.6
J5	90*	90*	?

*inferred from field observations

The ubiquitous joints exhibit fresh, unaltered and uneven surfaces with typical JRC value of 13. The joint wall compressive strength is evaluated at JCS = 40 GPa (Schmidt hardness of 31). The residual friction of the joints was estimated using tilt tests on saw-cut surfaces and is assumed to be 37°. The peak friction angle according to the Barton and Choubey criterion [10] ranges from 67° at the base of the cliff to nearly 80° at the top of the cliff, depending upon the value of the horizontal (normal) stress.

The ubiquitous joints are of a limited extent either vertically or laterally, as clearly seen in Figure 1. The joints that strike parallel to the free surface however are expected to have the most significant effect on overall cliff stability. The face parallel system was detected on both sides of the analyzed segment of the cliff, but is obscured behind the exposed face. The face parallel set is also unique in its persistence, continuity, and relatively open configuration. In places the openings reach several tens of centimeters; this is in contrast with the characteristics of the other sets of joints.



Fig. 1. General view of the cliff.

2.1. Kinematical considerations

Kinematical analysis performed using Block Theory [11] shows that removable key-blocks are formed by the following joint combinations: $JC1 = J_1J_2J_3$; $JC2 = J_1J_2J_4$; $JC3 = J_2J_3J_4$. The factor of safety (F.S.) for these blocks is 0.18 for JC1 against sliding on $I_{2,3}$ (intersection line of J_2 and J_3), F.S. = 0.04 for JC2 against sliding on $I_{2,4}$ and F.S. = 0.04 for JC3 against sliding on $I_{2,3}$. The blocks formed by these joint combinations are slender tetrahedral prisms because the line of intersections along which failure develops is sub-parallel to the free surface. Such removable key-blocks have been named "non-

hazardous" [12] because although removable, the volume of the block will be very small and consequently the associated risk minimal. Under similar considerations toppling of individual blocks is ignored. The open, persistent, face parallel tensile cracks however imply that rotational instability is active within the rock mass.

2.2. Mechanical considerations

The cantilevered geometry of the studied cliff leads to eccentric loading of gravity forces with respect to the centerline of the base. In a continuous rock mass such eccentric loading will induce tensile stresses when the load resultant lies outside the section's kernel. However the studied rock mass is transected by a multitude of discontinuities, which can not resist tensile stresses. Consequently, the eccentric loading causes opening across the discontinuities. Since large, face parallel, vertical tension cracks are found within the rock mass, a large scale, forward slope rotation is anticipated due to lack of tensile strength capacity across joints and beddings. The size and location of the section's kernel, and the amount of rotation, are all determined by the depth of the vertical tension crack, the height of the cliff and the exact geometry of the overhanging slope.

In addition to face parallel joints, normal faulting typical to regional geology has been considered. Most known normal faults in the region are dipping by 55° to 75° . Faults can be considered as stable end product of all possible mechanical regimes the mass of rock has been gone through, and therefore should be considered as possible detachment plane located at the back of the cliff. Assuming a fault plane dipping by 70° , commencing at the base of the cliff, the expected termination at the surface of the cliff is to be found at about 10m from cliffs edge.

To account for the uncertainty with respect to the depth of the face parallel tensile crack or the location of a normal fault, five different scenarios are modeled: tension crack at a distance of 5m, 10m, 15m, 20m and 25m from the toe. For easy of comparison both joints and faults were modeled as vertical planes with zero tensile strength and cohesion. Rock mass parameters, determined using standard laboratory test, has been considered to be of a minor influence to the paramount influencing factor of the parallel joint.

3. CONTINUUM MECHANICS STABILITY ANALYSIS

A study of the behavior of the overhanging cliff is first conducted using a continuum mechanics approach. The rock mass is considered continuous and not jointed. It has free boundaries formed by a vertical “tension crack” on the back of the cliff and by its sloped façade.

The simulation is carried out with the STRAP [13] FEA program. A typical model is presented in Fig. 2. The rock is presented by a 2D-plane strain linear-elastic constitutive law. The elements used are the Pian-Sumihara 4-node hybrid quadrilateral elements [14]. The element mixed formulation is based on the Hellinger-Reissner variational principle derived from the following functional:

$$\Pi_R = \int_V \left[-\frac{1}{2} \boldsymbol{\sigma}^T \mathbf{s} \boldsymbol{\sigma} + \boldsymbol{\sigma}^T (\mathbf{D} \mathbf{u}_q) - (\mathbf{D}^T \boldsymbol{\sigma})^T \mathbf{u}_\lambda \right] dV \quad (1)$$

The elements displacements are decomposed into two parts such that

$$\mathbf{u} = \mathbf{u}_q + \mathbf{u}_\lambda \quad (2)$$

where \mathbf{u}_q are compatible displacements in terms of nodal displacements and \mathbf{u}_λ are internal displacements which may be compatible and incompatible. $\mathbf{D}^T \boldsymbol{\sigma} = 0$ are the homogeneous equilibrium equations and the last term in the integral is the Lagrange multiplier term to impose such constraints.

The essential terms of the assumed stresses are expanded as complete polynomials in the natural coordinates of the element. The equilibrium conditions are imposed in a variational sense through the internal displacements that are also expanded in the natural coordinates. A small perturbation method is used to determine the equilibrium constraint equations.

The base of the cliff is supported on uni-directional springs, namely springs that follow a linear Hookean constitutive law in compression only. No tension forces are allowed in the springs and therefore gaps may open at the base. This “no tension” constraint leads eventually to a solution of non-linear equations.

The mesh is composed of 1.0m x 1.0m elements. Young’s Module of Elasticity is taken as 70 GPa for the rock. Poisson’s ratio is taken to be 0.25.

Unidirectional springs are attached to each of the nodes at the bottom of the mesh. The spring’s stiffness represents a Subgrade reaction coefficient of $7.5 \cdot 10^8 \text{ N/m}^3$ i.e. they will allow 1.0 mm of settlement under a pressure of 0.75 MPa. Gravitational static load due to the self weight of the rock (taken as 25 kN/m^3) is applied in the FE analysis.

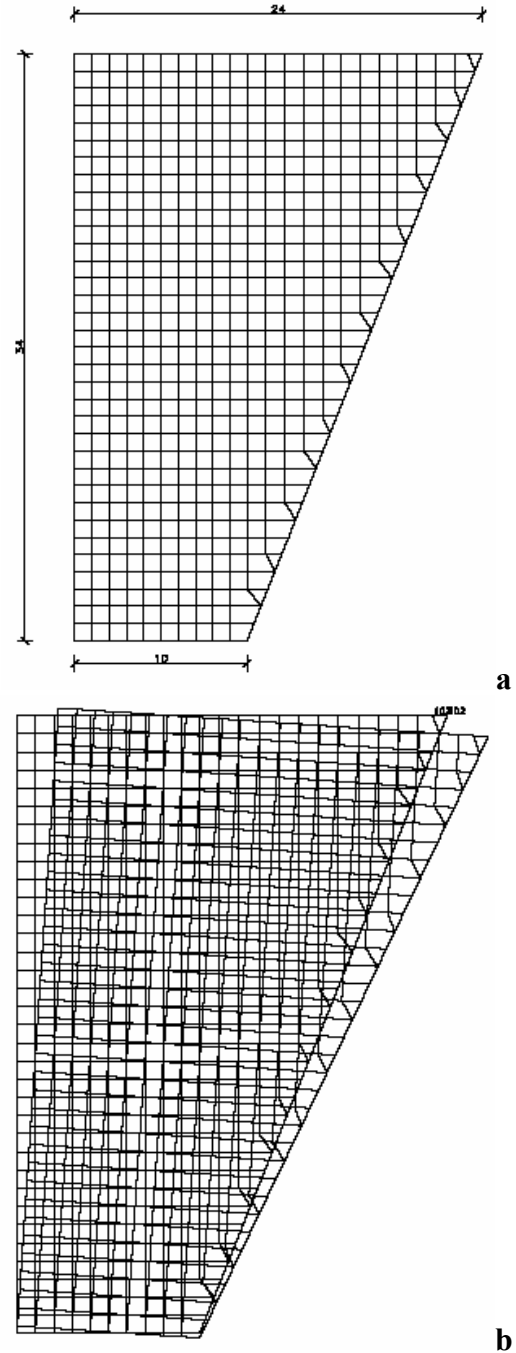


Fig. 2 .a) Finite element model with a vertical tension crack located 10m from its toe; b) the FEA deformed shape with a vertical tension crack located 10m from its toe.

The solution for the cliff with a tension crack that is located 5m from the toe became unstable. In that case the resultant of the self weight loading passes through a location that is external to the base.

The deformed shape of the cliff with a tension crack that is located 10m from the toe is shown in Fig. 2b. It is shown that the cliff rotates forward almost as a rigid body. This is due to the asymmetric shape of the cliff. The resultant of the self weight is eccentric with respect to the centerline of the base. Therefore the base contact stresses that develop are not uniformly distributed and consequentially the vertical displacement of the base is not uniform along the base. A horizontal displacement of 102 mm and a vertical displacement of 52 mm develop at the top. A gap is formed at the base of the cliff. The gap length is 6.5 m. This leaves only 3.5 m of the base in contact, and produces linearly varying contact stresses with a maximum value of 7.9 MPa at the toe.

The cliff with a tension crack that is located 20 m from the toe demonstrates a horizontal displacement of 6mm only at its top. So is the vertical displacement there. In that case the eccentricity of the resultant of the self weight loading is much smaller than in the former example, and passes within the kernel of the base. No gap is formed at the base of the cliff and the maximum contact stress is 2.5 MPa.

It is seen that even though a continuum mechanics approach is not generally suitable for the analysis of discontinuous rock masses, it can provide us with some insight to the overall stability problem. It is often good practice to use relatively simple and robust computational tools before performing rigorous complex analysis.

4. DISCONTINUOUS STABILITY ANALYSIS

Fully discontinuous analysis is performed using the implicit member of the DEM family: the Discontinuous Deformation Analysis - DDA [9]. DDA models a discontinuous material as a system of individually deformable blocks that move independently without interpenetration. In the DDA method the formulation of the blocks is very similar to the definition of a finite element mesh. A finite element type of problem is solved in which all elements are physically isolated blocks, bounded by pre-existing discontinuities. The blocks used in DDA can assume any given geometry, as opposed

to the predetermined topologies of the FEM elements.

In DDA individual blocks form a system of blocks through contacts among blocks and displacement constrains on a single block. For a block system defined by n blocks the simultaneous equilibrium equations are $\mathbf{KD} = \mathbf{F}$ where \mathbf{K} is the global stiffness matrix, \mathbf{D} is the displacement variables vector and \mathbf{F} is the forcing vector. The total number of displacement unknowns is the sum of the degrees of freedom of all the blocks. The simultaneous equations are derived by minimizing the total potential energy Π of the block system [9].

The solution to the system of simultaneous equilibrium equations is constrained by inequalities associated with block kinematics, i.e. no penetration and no tension condition between blocks. The kinematical constrains on the system are imposed using the penalty method. Shear displacement along the interfaces is modeled using Coulomb - Mohr failure criterion. The large displacements and deformations are the accumulation of small displacements and deformations at each time step.

The accuracy of DDA for slope stability problems has been tested by many researchers, using analytical solutions for static and dynamic problems, physical models, and case studies. For an extensive summary of DDA validation see MacLaughlin and Doolin 2005 [15].

4.1. Gravitational loading

DDA analysis is performed for five different geometrical configurations, where the depth of the “tension crack” is modeled at: 5m, 10m 15m, 20m and 25m from the toe, referred to herein as Cases 1 to 5 respectively. The mechanical properties of the rock mass, numerical control parameters and modeling cases are given in Table 2. The DDA undeformed geometry of Case 1 is shown in Figure 3a.

The displacements within the rock mass are recorded at 8 different measurement points (mp) within the rock mass: 4 points in front of the “tension crack” and 4 points within the rock mass behind the “tension crack”. The x,y locations of the measurement points with respect to an origin set at the base of the “tension crack” are given in Table 3, and are shown in Figure 3a.

Table 2. Mechanical properties of the rock mass, DDA numerical control parameters and cases modeled.

Rock mass properties	
Dry specific weight	24.54 kN/m ³
Elastic Modulus	70 GPa
Friction angle along interfaces	41°
DDA numerical control parameters	
Time step size	0.0005sec
Assumed maximum displacement within time step*	0.001
Contact normal stiffness	7.5 · 10 ⁸ N/m
Inter-step velocity coefficient	0.98
Modeling cases	
Case 1	5m from toe
Case 2	10m
Case 3	15m
Case 4	20m
Case 5	25m
Case 6	5m dynamic input
Cases 7, 8, 9	5m with $\phi = 1''$, $\phi = 2''$ and $\phi = 3''$ rock bolts

Figure 4 shows the relative displacements (u, v) recorded at the different measurement points for Case 1. The top extremity of the cliff ($mp1$) undergoes negative vertical displacement (v) and a positive horizontal displacement (u). The equivalent measurement point at the same height but 18.14m behind the face ($mp2$) undergoes positive displacements in the horizontal and vertical directions. These two points are located at the two ends of a horizontal segment, which marks the top of the cliff. The recorded displacements indicate that the rock mass in front of the tension crack is rotating forward.

Table 3. Location of the measurement points in the DDA mesh of Case 1

	Location (x, y) m	Remarks
Origin	0,0	base of tension crack
mp1	18.14, 35.54	Cliff top
mp2	0.1, 35.54	
mp3	0.1, 0	
mp4	5,0	Cliff toe
mp5	-0.1, 35.54	
mp6	-19.9, 35.54	
mp7	-19.9, 0	
mp8	-0.1, 0	

The measurement points at the base of the rotating mass show very little displacement, thus indicating that the center of rotation is found at some height above the base of cliff. The graphic output (Fig. 3b)

clearly shows the numerical results: the horizontal opening of the tension crack is reduced from top to bottom and is negligible at a depth of 29m from the surface.

The displacements within the rock mass behind the tension crack are very small when compared with the displacements of the rotating mass. The horizontal displacements are smaller by two orders of magnitude, and the vertical displacements are smaller by one order of magnitude, indicating that the rock mass behind the tension crack is static and stable.

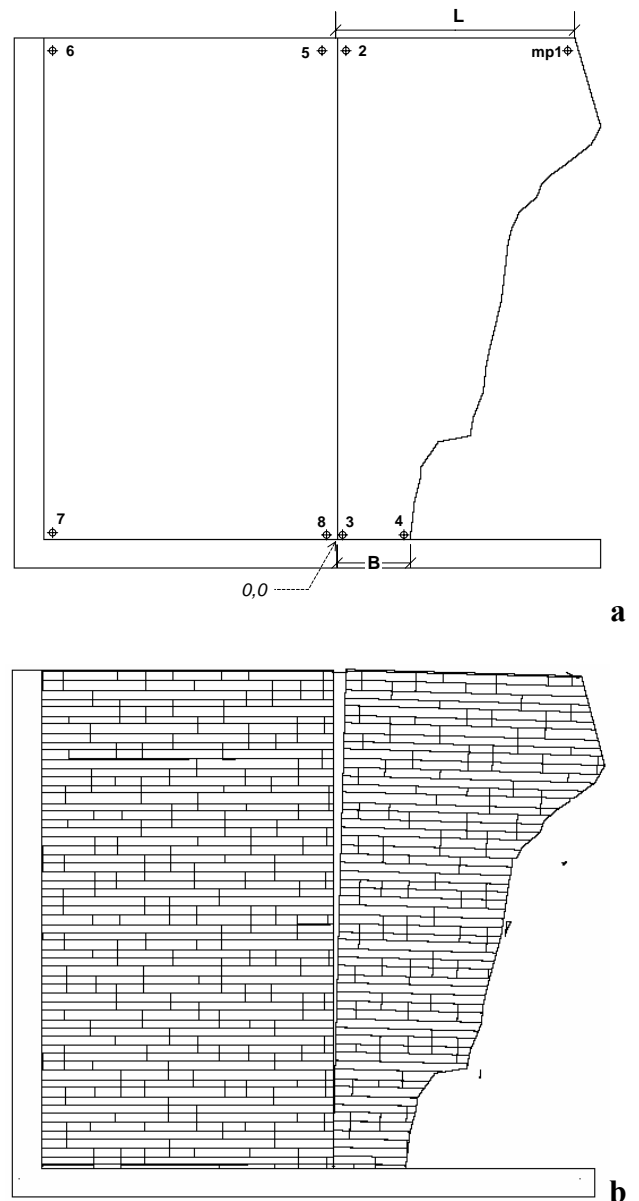


Fig. 3. DDA Case 1 model: a) undeformed shape and location of measurement points – no joints are shown; b) deformed shape after 20 seconds.

When the tension crack is located at a depth of 10m with respect to the toe (Case 2) the displacements

are restrained when compared with Case 1 however the trend is similar to the described above for Case 1. Figure 5 shows time histories of horizontal displacements (u) for the different cases. It is clear that only for the 5m case (Case 1) the cliff undergoes unrestrained deformation. For the other four cases the displacements are arrested at approximately 20% of total computed time (4 sec) with the exception of the 10m case where displacement arrest is detected at 50% of total time (10 sec).

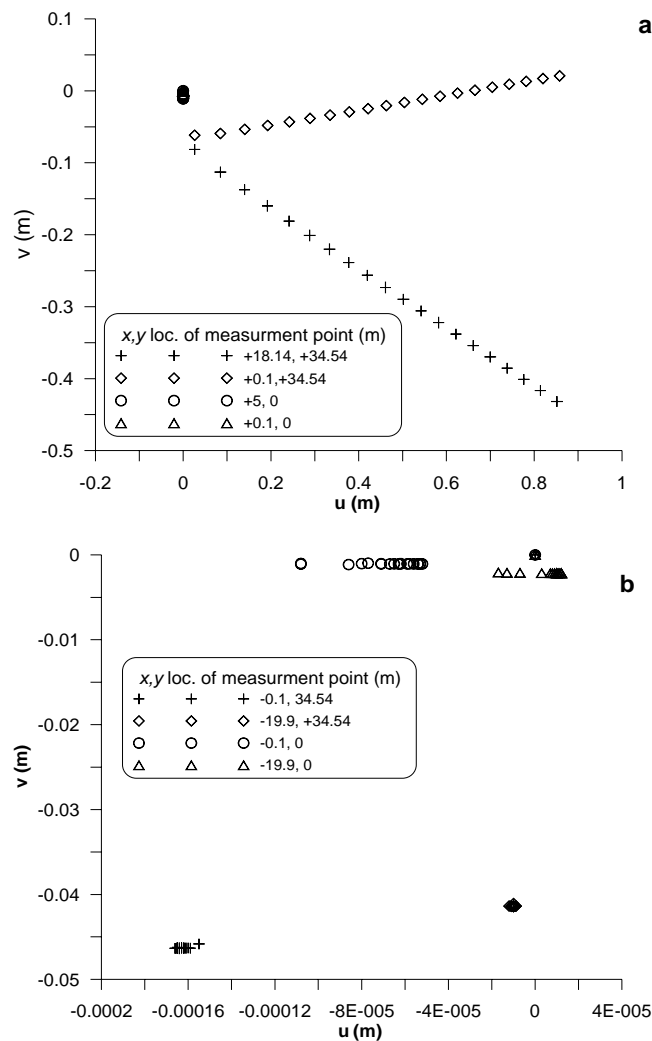


Fig. 4. Vertical displacement (v) vs. horizontal displacement (u) for DDA Case 1: a) displacements in front of the vertical tension crack; b) displacement behind the vertical tension crack.

4.2. Dynamic loading

Dynamic analysis is performed by applying time dependent accelerations to the block system forming the cliff using the seismic record of the 1995 $M_w = 7.1$ Nuiweba earthquake. In order to attain computational efficiency the full 50 sec record of the earthquake is trimmed to contain the

critical 10.5 sec of the record (Fig 6). The Peak Horizontal Ground Acceleration (PGA) of the record is 0.05g. Additional dynamic analysis is performed using the same seismic record but scaled to produce $PGA = 0.25g$. According to the Israeli Code of Building [16] the expected PGA in the area is 0.179g.

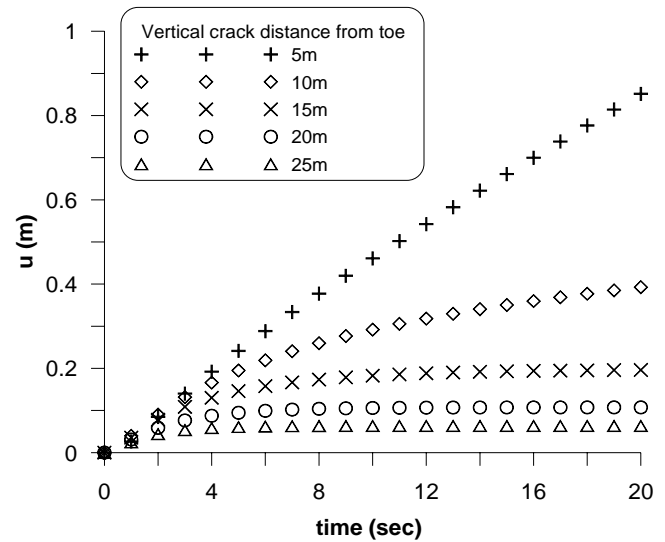


Fig. 5. DDA time histories of the horizontal displacements (u) of $mp1$ for Cases 1 to 5.

Figure 7 shows the displacement components (u, v) at the top extremity of the cliff ($mp1$), for Case 1 geometry subjected to different loading scenarios: 1) gravitational loading; 2) seismic loading; 3) seismic loading scaled up by a factor of 5. It is clearly seen that the magnitude of displacements and their pattern are essentially identical: the displacement components are increased by only 2.5% due to the up-scaled seismic load. It can therefore be concluded that the static case (gravitational load only) represents the critical state of cliff stability, and that the effect of seismic loads is of minor importance.

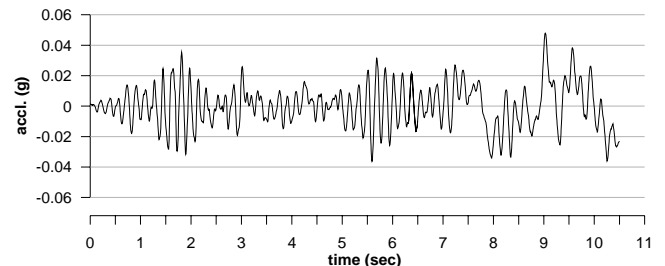


Fig. 6. Dynamic input motion for DDA models.

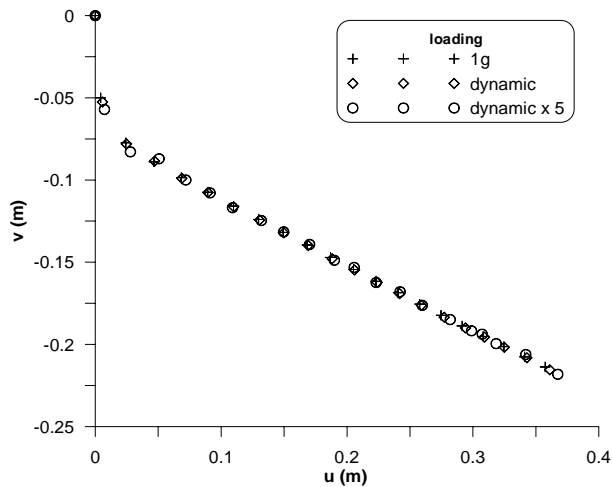


Fig. 7. DDA time histories of the horizontal displacements (u) of $mp1$ for Cases 1: gravitational and seismic loading.

5. ROCK BOLT REINFORCEMENT

The stability analysis of the studied cliff indicates that rotational failure ensues when the depth of the face parallel tension crack is up to 5m from the toe of the discontinuous cliff. When the depth of the tension crack is greater the cliff is stable. Based on these findings rock bolt reinforcement is added to the DDA model. The bolts are vertically spaced 4m apart, from bottom to top (Figure 8). The individual bolt length is adjusted such that the static end of the each bolt is anchored 3m behind the tension crack.

The stiffness (k) of each bolt is given by: $k = \frac{E \cdot \pi \cdot \phi^3 / 2}{L}$, where E is Young modulus for steel, ϕ is bolt diameter, and L is bolt length. Three different bolting simulations are performed for varying bolt diameters: $\phi = 1''$, $\phi = 2''$ and $\phi = 3''$ and therefore varying bolt stiffness.

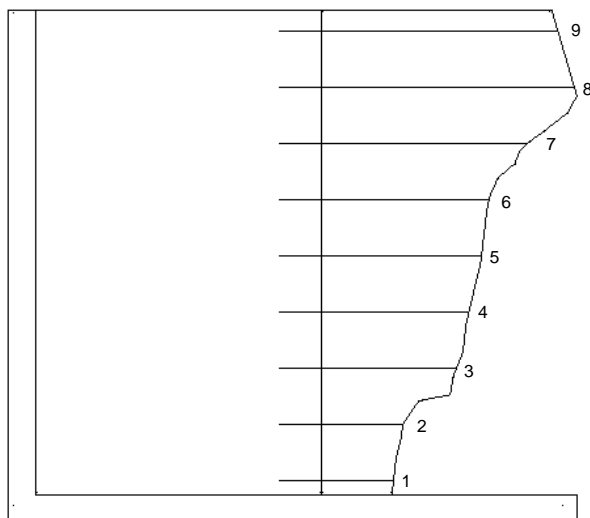


Fig. 8. DDA domain boundary of Case 1 with rock bolts.

Figure 9a shows time histories of the horizontal displacement component at the top of the cliff ($mp1$) as a function of modeled bolt diameter. The upper bound for top cliff displacement is represented by the displacements calculated for an unsupported cliff - Case 1; while the lower bound is represented by the displacements calculated for Case 5 geometry. Clearly, the slope displacement components are reduced with increasing bolt diameter (or stiffness). It is found that complete slope stabilization is obtained with bolt diameter of 2" and above. With a bolt diameter of 1" slope displacements are never arrested and the cliff is rendered unsafe. With bolt diameters of $\phi = 2''$ and $\phi = 3''$ the horizontal slope displacements at $mp1$ are 0.29m and 0.19m respectively (Figure 9b).

Plotting the ultimate horizontal displacement (u) at $mp1$ against bolt diameter (Figure 9a) shows that the two are related through a simple exponential law: $u = 0.9e^{-0.52\phi}$. Using this function the displacement for other possible bolt diameters can be assessed with high degree of accuracy for the studied overhanging slope.

The bolt axial forces (F_B) as computed by DDA are presented in Figure 10 where the x - axis represents the vertical position of each rock bolt. We find that maximum axial force changes with diameter and vertical position, $F_B (\phi = 1'') = 147 \text{ kN}$ at bolts number 6 and 9; 2) $F_B (\phi = 2'') = 237 \text{ kN}$ at bolts number 6 and 9; and 3) $F_B (\phi = 3'') = 309 \text{ kN}$ at bolt number 6.

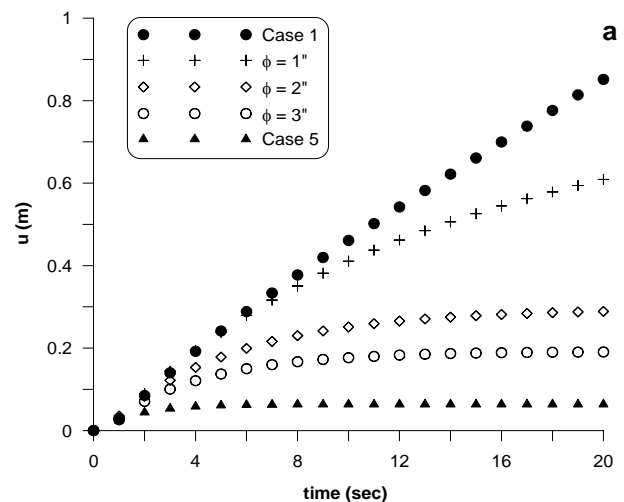


Fig. 9. a) DDA time histories of the horizontal displacements (u) of $mp1$ for Cases 1 for different values of rock bolts diameter.

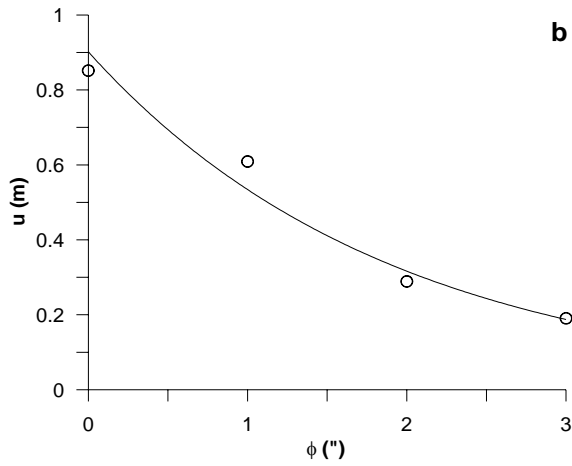


Fig. 9.(cont.) b) ultimate displacement of $mp1$ as a function of rock bolt diameter.

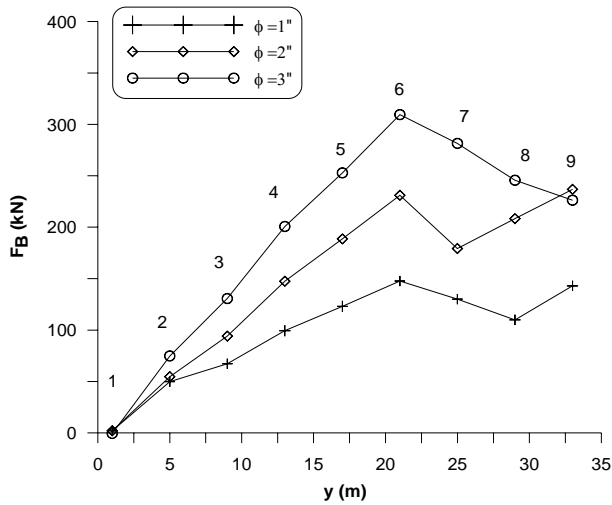


Fig. 10. Axial force in rock bolts for different values of rock bolts diameter.

6. DISCUSSION

The stability of an overhanging cliff with vertical joints and horizontal beds is studied using three different approaches: 1) key-block theory; 2) continuous FEA; and 3) DDA. Block theory analysis shows that local failure of tetrahedral blocks can take place. However, these local failures have little impact on the overall cliff stability. This conclusion is supported by field evidence where very few slender moulds of failed keyblocks were mapped along the face.

The stability of the cliff is primarily controlled by two factors: 1) the cantilevered geometry of its face and 2) the depth of the face parallel, vertical tension crack. Since the face geometry is known, it is the location of the tension crack that controls overall cliff stability. In this paper we apply both continuous and discontinuous numeric approaches in an increasing order of complexity. First a

relatively simple and robust continuous FEA is executed, thus providing a first order approximation of cliff behavior. The insights gained from FEA are then incorporated in to DDA, thus the model is further refined. Finally, a fully discontinuous model with rock bolt reinforcement is analyzed, and the influence of rock bolting on cliff stabilization is determined.

Both FEA and DDA predict that the cliff is instable when the vertical tension crack is at a depth of 5m from the toe. The mode of failure is essentially the same, forward rotation. The numerical values of the displacement however are not comparable because DDA is fully dynamic and the deformation evolves with time. However, when DDA's deformation reaches equilibrium the displacements are comparable (Table 4). Taking as an example Case 2 (with face parallel crack 10m from toe) it can be seen that while in FEA the entire mass rotates as a rigid body around a point located at the base of the mass, in DDA the rotation is taking place 5m above the base. The numerical values of displacement are 0.102m and 0.39m respectively. The discrepancies between the calculated displacements in the two methods are due to the governing constitutive relations of each method. While in the continuous FEA the tensile stresses due to eccentric loads are compensated by vertical displacements at the base, in the discontinuous DDA these tensile stresses are compensated by vertical displacements across bedding planes. The net displacement in DDA is the sum of individual displacements across the bedding planes.

Table 4. Comparison of MP1 horizontal displacement for different analysis method. B is depth of vertical crack from cliffs toe.

B	FEA	DDA w/o joints	DDA
10m	0.102m	0.05m	0.39m
20m	0.006m	0.019m	0.11m

It is interesting to note that the displacements in DDA without systematic joints are close to those of the FEA: 0.05m compared with 0.1m respectively for Case 2 and 0.019m compared with 0.006m respectively for Case 4. These differences are attributed to absence of internal discretization of the DDA domain when modeling the rock mass as a single continuous block. In DDA each block, irrespective of size, is modeled as a simply

deformable body, the net deformation of a rock mass is the sum of individual intra-block deformation and inter-block displacements.

The presented case study can be further generalized to address the broader problem of overhanging cliffs. Clearly the eccentricity of loading, and consequently the rotational instability, is determined by the ratio between the length of the base (B) and the length of the top surface (L) of the rotating mass (refer to Figure 3a). Figure 11 shows the relation between the horizontal displacement component u of the cliff extremity normalized by the displacement of Case 1 ($u/u_{B=5m}$) to the ratio B/L ratio. This ratio can be used as an index for the degree of eccentricity at the base of the cliff. As B/L ratio approaches unity the eccentricity of loading diminishes until the slope is homogeneously loaded under its own weight. Where B/L ratio is lower than 0.4 the cliff is assumed to be unstable. Naturally, different slope angles will result in somewhat different numeric values of B/L ; the general behavior however is expected to follow similar trend.

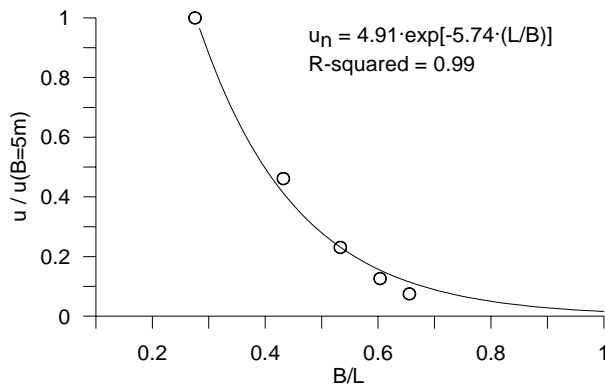


Fig. 11. Normalized horizontal displacement of mpl as a function of B/L ratio.

The ever-growing reliance on computational schemes, such as FEA or DDA, requires rigorous control over the numeric accuracy of the solution. This is typically achieved by validations using analytical solutions or physical models. However, no analytical solution or laboratory model can duplicate the scale and character of the loading, boundary and environmental conditions inherent to full-scale problems. Furthermore, in discontinuous rock masses the spatial arrangement of the discontinuities is complex, and in times only partially attainable. Therefore, comparison between numerical predictions and actual behavior using real case studies can help insure that extrapolation from

simple problems to field scale problems is basically valid.

DDA predicts that the cliff is stable when the vertical tension crack is located 10m from the toe or deeper. The amount of opening across the vertical crack reaches 0.4m, which is within the order of magnitude of opening measured along the tension cracks in the field. This implies that for the overhang analyzed in this study the face parallel tension crack should be located at a depth of 10m from the toe. This estimate supports the measured inclinations of normal fault planes or vice versa – the field measurement of fault planes supports the predictions made by the DDA method.

Instability and failure must ensue when the tension crack is found 5m from toe; or when a normal fault with steeper inclination transects the slope. The proposed stabilization scheme caters for both numerical model and field observations, by addressing the critical depth of the tension crack at 5m. The proposed rock bolts are anchored beyond this depth and the bolt stiffness values are set to prevent excessive displacements.

7. CONCLUSIONS

1. Vertical rock cliffs transected by vertical joints and horizontal bedding planes are stable. Local failures of removable rock blocks may occur, however, these instabilities have little impact on the overall cliff.
2. The stability of vertical rock cliffs transected by vertical joints and horizontal bedding planes is compromised where overhangs cantilever above the base of the cliff, thus subjecting the rock mass to eccentric loading with respect to the centerline at the base.
3. The stability of eccentrically loaded overhanging cliffs is determined by the depth of the face parallel tension crack found at the back of the cliff. In this research it is found that an eccentrically loaded 34m high cliff is unstable for $B/L < 0.4$.
4. Both FEA and DDA correctly predict the mode of failure. However, the continuous FEA do not provide the exact nature and amount of deformation.
5. It is suggested that a robust FEA model should be used as a preliminary analysis tool, and then

the insights gained may be incorporated in a refined DDA model.

6. It is shown that a thorough geological reconnaissance can provide constructive insights with respect to the geometry and the assumptions of numerical modeling. The current research proves that structural geology concepts and findings could be used jointly with modern analytical methods mutually supporting one the other.

8. ACKNOWLEDGMENTS

This research was funded by the Office of Geotechnical & Foundation Engineering, Administration of Planning and Engineering, Ministry of Construction & Housing – Israel. Gony Yagoda of the Department of Geological and Environmental Sciences at BGU is thanked for assistance with field survey and analysis of the structural data.

REFERENCES

1. Hoek, E. 2000. *Practical Rock Engineering – Course Notes*. <http://www.rocscience.com/hoek/>.
2. Goodman, R. E and Kiefer, S. D. 2000. Behavior of rock in slopes. *J. of Geotechnical and Geoenvironmental Eng.* ASCE. 126 (8): 675-684.
3. Janbu N.1954. Application of composite slip surfaces for stability analysis. *European Conference on Stability of Earth Slopes*. 3:43-49.
4. Bishop A.W. 1955. The use of the slip circle in the stability analysis of slopes. *Geotechnique*.1:7-17.
5. Wittke, W. 1965. Methods to analyze the stability of rock slopes with and without additional loading. *Rock Mechanics and Engineering Geology*, supplement 2, Springer, Vienna.
6. Goodman, R. E., and Bray, J.W. 1977. Toppling of rock slopes. *Proc .Specialty Conf. on Rock Engrg. for Foundations and Slopes*, Vol. 2,ASCE, New York, 201-234.
7. Zhang, L. and Einstein, H. H. 1998. Estimating the mean trace length of rock discontinuities. *Rock. Mech. Rock. Eng.* 31(4): 217-235.
8. Mouldon, M. 1998. Estimating mean fracture trace length and density from observations in convex window. *Rock. Mech. Rock. Eng.* 31(4): 201-216.
9. Shi, G-h. 1993. *Block System Modeling by Discontinuous Deformation Analysis*. Topics in Engineering Vol. 11, Computational Mechanics Publications. 209p.
10. Barton, N.R. and Chaubey, V., 1977, The shear strength of rock joints in theory and practice, *Rock. Mech. Rock. Eng.* 10: 1-54.

11. Goodman, R. E. and Shi, G-h. 1985. *Block theory and its application to rock engineering*. Prentice. Hall, New Jersey. 338p.
12. Hatzor, Y.H. and Feintuch, A. (in press) The joint intersection probability. *Int. J. of Rock Mech. and Min. Sci.*
13. STRAP Ver. 11.0. 2004. Structural Analysis Program. ATIR Engineering software Development Ltd., Israel,
14. Pian T.H.H. and Sumihara K., 1984. Rational Approach for Assumed Stress Finite Elements. *Int. J. Num. Methods Eng.* 20: 1685-1695.
15. MacLaughlin, M. M. and D. M. Doolin. 2005. Review of validation of the Discontinuous Deformation Analysis (DDA) method. *Int. J. Numer. Anal. Meth. Geomech.* 29
16. Code 413. 2004. Design provisions for earthquake resistance of structures, Revision 2. Israel Institute of Standards.